Assessment of aquifer vulnerability in the tectonically deformed sedimentary rocks in Abakaliki area, southeastern Nigeria, using geophysical and geological data

Ikenna A. Obasi (ikenna.obasi@fulokoja.edu.ng)
Federal University Lokoja
Jamilu B. Ahmed II
Federal University Lokoja
Godwin O. Aigbadon
Federal University Lokoja
Emmanuel K. Anakwuba
Nnamdi Azikiwe University
Ernest O. Akudo
Federal University Lokoja
Nneka M. Onwa
University of Calabar

Research Article

Keywords: Aquifer, Vulnerability, Abakaliki, Fractured rocks, Nigeria

Posted Date: July 5th, 2022

DOI: https://doi.org/10.21203/rs.3.rs-1725870/v1

Abstract

A combination of the IEC, AVI, and GOD pollution indices were used to assess the vulnerability of the fractured rock aquifer in the Abakaliki area to pollution from anthropogenic sources. The topsoil ranges from laterite to silt to silty-clay, according to the results of the vertical electrical sounding (VES). The geoelectric sections have varying numbers of layers (1–6 layers) with their resistivity ranges as 29.16–3,949.30 Ω, 4.98–1,630.70 Ωm, 0.35–3,767.20 Ωm,1.76–7926.30 Ωm, and 1.11–3,060.20 Ωm respectively. These have been grouped into four main lithologic units namely the topsoil, indurated/baked shale, fractured shale/sandstone (the aquiferous unit), and the consolidated sandstone units. The thickness of the vadose zone is generally thin (< 18 m), while their hydraulic conductivity is relatively high (0.20–16.11 m/day) for argillaceous rocks. The IEC values (0.003–0.850 *S*) suggest a weak to fair protective capacity for the vadose zone. The result of the *HR* (1.01–55.49) indicates that the underlying aquifer is highly to extremely vulnerable, and the GOD values (> 0.7) agree that they are extremely vulnerable.

1.0 Introduction

The role of groundwater as a global source of freshwater is quite known (Famiglietti 2014). The only supposedly safe means of supply of potable water in the Abakaliki area is the groundwater (Obasi et al. 2021). It has, however, not yet been ascertained how safe the groundwater is by evaluating the protective capacity of the geological materials overlying the zone of groundwater occurrence. Recent studies indicate that there are contaminants in surface waters, which may as well infiltrate into the groundwater system if the overlying geological materials permit their smooth transmission (Ebokaiwe et al. 2018). The contaminants are partly geogenic and partly from anthropogenic sources, especially the mining of sulphide ores and quarrying of shales and pyroclastics in the Abakaliki area (Omaka et al. 2017, Obasi et al. 2020). The contaminants can be transported to the aquifer systems in the study area through either advection, dispersion, or diffusion (Ezzy et al. 2006). The degree of infiltration is a function of the thickness and permeability of the vadose zone (Foster et al. 2002; Akpan et al. 2015). Shallow-seated aquifers with thin vadose zone are highly susceptible to pollution (Okiongbo and Akpofure 2012).

Groundwater vulnerability is not measured directly (Akpan et al. 2015), however, it can be measured using analogue models and parametric systems (Conrad et al. 2002). Different methods that have been previously applied in assessing aquifer vulnerability include the DRASTIC (Aller et al. 1987; Leone et al. 2009; Javadi et al.2011), the Aquifer Vulnerability Index (AVI) (Draoui et al. 2007; Ducci and Sellerino 2012; Fraga et al. 2013; Edet 2014), the Integrated Electrical Conductivity (IEC) (Kirsch et al. 2003; Casas et al. 2008), the groundwater hydraulic confinement–overlying strata–depth to water table (GOD) (Foster 1987; Foster et al. 2002) and SINTACS (Civita and De Maio 1997; Sinkevich et al. 2005; Yin et al. 2012) methods. The advantage of integrating the IEC and the GOD techniques over the other techniques is their ability to generate a result of high efficacy from few numbers of data (Draoui et al. 2007; Fraga et al. 2013; Akpan et al. 2015).

The study area is dominated by fracture aquifer systems that are highly localized and lacks interconnectivity (Benkhelil 1989), within the Cretaceous shales, sandstones, mudstones, limestones, and volcaniclastics (Okeke et al. 1987; Chukwu and Obiora 2018) which are members of the Asu River and Eze-Aku Groups. These fracture systems are products of multiple tectonism that affected the area in Cretaceous times (Benkhelil 1989; Obiora and Charan 2011). The thickness of the vadose zone was estimated to be ≤ 18 m in most of the places (Obasi et al. 2021). The hydraulic properties of the vadose zone have not been measured previously to ascertain their protective role to the aquifer systems in the area. Groundwater is the primary source of potable water in the study area (Onwa and Obasi, 2022). Having such a shallow-seated aquifer system, there is a need to evaluate the aquifer's vulnerability. The aim of this paper, therefore, is to access the vulnerability of the groundwater in the study area to contaminants using the integrated electrical conductivity (IEC), the Aquifer Vulnerability Index (AVI), and the groundwater hydraulic confinement overlying strata depth to water table (GOD) techniques.

2.0 Site Description And Geologic Setting

The study area lies within Latitude $05^0$50'00" N–$06^0$40'00" N and Longitude $07^0$40'00" E–$08^0$30'00" E (Fig. 1). It is in the southern portion of the Benue Trough of Nigeria. Sediments were deposited in the basin in three main tectonic phases (Murat 1970). The first phase took place from Albian to Coniacian times. It resulted in the deposition of sediments of the Asu River Group (Albian), Eze-Aku Group (Turonian), and Awgu Formation (Coniacian), in the study area. The Santonian tectonism intruded the host rocks with some volcaniclastics and intermediate igneous rocks (Benkhelil 1989; Chukwu and Obiora 2014; 2018). The Santonian tectonic event diagenetically altered the host rocks, and replaced their primary aquiferous properties (Obasi and Selemo 2018) with some structural aquifer systems such as fissures, fractures, joints, faults and weathered zones (Ebong et al. 2014).

3.0 Research Method

Vertical electrical sounding (VES) was carried out at 40 locations in the study area using the Schlumberger electrode configuration. The Petrozenith resistivity metre was applied in this study with 2 pairs of electrodes, 2 pairs of cable reels, a Global Positioning System (GPS), a Direct Current Source (Dry Cell batteries), survey datasheets, and measuring tapes. The half current electrode separation (AB/2) ranged from 1–100 m and the potential electrode spacing ranged from 0.25–10 m (Lowrie 2007). The field results were recorded and later plotted as graphs using the Interpex IX1D software. This enabled the generation of the geoelectric sections of the subsurface layers (Table 1).

Table 1
Geoelectric section and lithologic description of the subsurface.

VES NO	Geoelectric layers	Apparent Resistivity (Ωm)	Thickness (m)	Depth (m)	Inferred Lithology	Curve Type
1	1	289.36	0.5	0.5	Top soil	K
	2	297.88	6.99	7.5	Shale	
	3	50.41	104.14	111.63	Fractured shale	
	4	5475.6			Sandstone	
2	1	91.12	0.24	0.24	Top soil	K
	2	131.97	0.21	0.45	shale	
	3	309.74	7.62	8.07	shale	
	4	40.32			Fractures shale	
3	1	6253.5	0.35	0.35	Sandstone	HK
	2	128.13	0.64	0.99	Shale	
	3	3767.2	3.71	4.7	Sandstone	
	4	12.55	10.07	14.78	Fractured shale	
	5	956.89			sandstone	
4	1	64.56	0.64	0.64	Top soil	HK
	2	68.6	13.11	13.76	shale	
	3	29.85	29.07	42.82	Fractured shale	
	4	230.36			shale	
5	1	239.41	1.44	1.44	Top soil	HK
	2	78.37	5.3	6.74	shale	
	3	7388.2	0.21	6.96	sandstone	
	4	23.39	10.23	17.19	Fractured shale	
	5	4645			sandstone	
6	1	268.37	0.32	0.32	Top soil	HQ
	2	67.24	10.59	10.91	Shale	
	3	12.07	11.37	22.27	Fractured shale	
	4	146.42			shale	
7	1	148.67	0.51	0.51	Top soil	Q
	2	119.64	4.17	4.68	shale	
	3	18.12	26.69	31.37	Fractured shale	
	4	7.38			Fractured shale	
8	1	101.84	2.31	2.31	Top soil	H
	2	0.21	0.11	2.42	clay	
	3	385.08			shale	
9	1	0.33	0.74	0.74	Top soil	HK
	2	67			Shale	
10	1	73.28	0.85	0.85	Top soil	HQ
	2	40.69	7.27	8.12	shale	
	3	0.35	0.92	8.22	clay	
	4	50.15	57.35	65.56	shale	
	5	11.86			Fractured shale	
11	1	81.46	0.79	0.79	Top soil	H

VES NO	Geoelectric layers	Apparent Resistivity (Ωm)	Thickness (m)	Depth (m)	Inferred Lithology	Curve Type
	2	24.63	30.75	31.55	Fractured shale	
	3	327.9			Shale	
12	1	228.15	2.22	2.22	Top soil	Q
	2	95.53	23.75	25.97	shale	
	3	32.73	34.74	60.71	Fractured shale	
	4	2245.8			Sandstone	
13	1	250.11	2.2	2.2	Top soil	Q
	2	36.5	169.22	171.42	Fractured shale	
	3	10.74			Fractured shale	
14	1	396.39	1.6	1.6	Top soil	HK
	2	10.44	0.43	1.64	Clay	
	3	570.47	3.26	4.9	Shale	
	4	179.37	20.68	25.59	shale	
	5	14.46	2.94	28.53	Fractured shale	
	6	1142			Sandstone	
15	1	29,156	0.32	0.32	Sandstone	HQ
	2	594.17	5.59	5.92	Sandstone	
	3	917.73	12.27	18.18	Sandstone	
	4	4.38	1.21	19.4	Fractured shale	
	5	549.69			Shale	
16	1	343.66	1.69	1.69	Top soil	Q
	2	372.09	7.77	9.46	Shale	
	3	97.48	127.28	136.74	Shale	
	4	1.76			Fractured shale	
17	1	1420.4	0.59	0.59	Top soil	H
	2	2192.5	1.12	1.72	Sandstone	
	3	1.98	0.18	1.73	clay	
	4	34.61	4.38	6.11	Fractured shale	
	5	2050.7			Sandstone	
18	1	140.58	0.78	0.78	Top soil	HK
	2	4734.7	0.37	1.15	Sandstone	
	3	128.07			Shale	
19	1	192.65	1.95	1.95	Top soil	H
	2	2.22	0.28	2.23	clay	
	3	258.55			shale	
20	1	182.6	2.12	2.12	Top soil	HQ
	2	6.79	3.28	5.4	clay	
	3	15,743	136.05	141.45	Sandstone	
	4	4.27			Fractured shale	
21	1	44.59			shale	K
22	1	78.14	1.01	1.01	Top soil	Q
	2	8.31	1.59	2.61	Shale	
	3	20.73	2.44	5.05	Shale	

VES NO	Geoelectric layers	Apparent Resistivity (Ωm)	Thickness (m)	Depth (m)	Inferred Lithology	Curve Type
	4	12.98	51.24	56.29	Fractured shale	
	5	5.89			Fractured shale	
23	1	99.38			Shale	H
24	1	242.1	1.46	1.46	Top soil	HQ
	2	67.47	1.25	2.7	Shale	
	3	0.66	0.24	2.95	clay	
	4	93.55	14.12	17.06	shale	
	5	9.27			Fractured shale	
25	1	328.53	1.01	1.01	Top soil	K
	2	123.1	4.47	5.48	Shale	
	3	3.86	1.34	6.81	Fractured shale	
	4	16554	143.32	150.14	Sandstone	
	5	10.25			Fractured shale	
26	1	1053.8	2.69	2.69	Top soil	HQ
	2	212.07	10.5	13.2	Shale	
	3	139.72	44.37	57.57	Shale	
	4	7926.3			Sandstone	
27	1	151.28			Shale	Q
28	1	177.91			Shale	HK
29	1	201.29	0.41	0.41	Top soil	HK
	2	1630.7	1.42	1.83	Sandstone	
	3	75.37			Shale	
30	1	304.19	3.57	3.57	Top soil	H
	2	18.84	8.25	11.82	Fractured shale	
	3	80.99			Shale	
31	1	191.08	2.1	2.1	Top soil	HK
	2	4.63	3.17	5.27	shale	
	3	39.41			Fractured shale	
32	1	491.56	1.12	1.12	Top soil	Q
	2	184.56	5.22	6.34	Shale	
	3	2.15	0.51	6.85	clay	
	4	112.11	22.25	29.1	Shale	
	5	1.11			Fractured shale	
33	1	303.19	1.38	1.38	Top soil	Q
	2	75.3	0.67	1.39	Shale	
	3	85.61	2.92	4.31	Shale	
	4	146.71	13.33	17.64	Shale	
	5	16.95			Fractured shale	
34	1	125.59	2.31	2.31	Top soil	HK
	2	161.89	6.37	8.68	Shale	
	3	11.77			Fractured shale	
35	1	535.53	1.2	1.2	Top soil	HK
	2	608.83	0.62	1.82	Sandstone	

VES NO	Geoelectric layers	Apparent Resistivity (Ωm)	Thickness (m)	Depth (m)	Inferred Lithology	Curve Type
	3	107.33			Fractured sandstone	
36	1	193.77	1.67	1.67	Top soil	H
	2	20	4.21	5.88	shale	
	3	34.45	38.14	44.02	Fractured shale	
	4	1480.6			Sandstone	
37	1	3949.3	0.88	0.88	Top soil	HK
	2	83.48	3.55	4.43	Shale	
	3	3.55	1.86	6.29	Fractured shale	
	4	36.82			Fractured shale	
38	1	445.32	0.32	0.32	Top soil	HK
	2	360.7	4.99	5.31	shale	
	3	48.18	36.66	41.97	shale	
	4	6039.6			Sandstone	
39	1	51,26			shale	H
40	1	1333.3	0.47	0.47	Top soil	H
	2	27.21	24.55	25.02	Fractured shale	
	3	2515.2			Sandstone	

A combination of the geoelectric sections and the borehole lithologic logs (lithologs) generated during the drilling of groundwater boreholes at some of the locations of the VES enabled the effective delineation of the thicknesses of the vadose zone across the study area (Fig. 2). Hence, the resistivity of the vadose zone (R_{VD}) was determined by calculating the mean resistivity of the layers above the aquifer zone, while the thickness of the vadose zone (h_{VD}) was determined directly by correlating the geoelectric section with the borehole lithologs generated during the drilling of the water wells (Fig. 2) (Obasi et al. 2021).

The IEC was calculated from the processed field data using Eq. 1(Casas et al.2008; Akpan et al. 2015). The permeability (k) of the vadose zone was calculated using Eq. 2 (Obiora et al. 2016; Raji and Abdulkadir 2020). The hydraulic resistance (HR) was calculated using Eq. 3 (Van Stempvoort et al. 1992; Akpan et al. 2015). The GOD parameters were calculated using numerical values (Foster et al. 2002; Akpan et al. 2015). The information on the geoelectric sections and their corresponding vulnerability parameters for each location are represented in Table 2, while the general vulnerability classes is represented in Table 3.

Table 2
The summary of geoelectric data and vulnerability parameters in the study area.

VES points		Latitude Longitude	ρ_1	ρ_2	ρ_3	ρ_4	ρ_5	ρ_6	h_1	h_2	h_3	h_4	h_5
1	Onueke Stadium, Ezza	6^0 10^{l} 57.9^{ll} 8^0 02^{l} 58.3^{ll}	289.36	297.88	50.41	5475.60	_-	-	0.5	6.99	104.14	-	-
2	Spera-in-Deo junction, Abakaliki	6^0 18^{l} 33.5^{ll} 8^0 06^{l} 05.3^{ll}	91.12	131.97	309.74	40.32	-	-	0.24	0.21	7.62	-	-
3	Evangel camp Okpoto	6^0 24^{l} 46^{ll} 7^0 52^{l} 00^{ll}	6253.5	128.13	3767.20	12.55	956.89	-	0.35	0.64	3.71	10.7	-
4	Onuogo Mebiowa, Okposi	6^0 01^{l} 34.2^{ll} 7^0 49^{l} 40.8^{ll}	64.56	68.6	29.85	230.36	-	-	0.64	13.11	29.07	-	-
5	Nwangbogo house, Iyiazu, Oshiri	6^0 07^{l} 51.5^{ll} 7^0 52^{l} 53^{ll}	65.72	36.65	145.69	160.89	-	-	0.54	3.04	23.67	-	-
6	Ogoachi, Okposi	6^0 02^{l} 7.9^{ll} 7^0 47^{l} 57.3^{ll}	268.37	67.24	12.07	146.42	-	-	0.32	10.59	11.37	-	-
7	Achioma Mebiowa, Okposi	6^0 01^{l} 06.6^{ll} 7^0 49^{l} 35.8^{ll}	148.67	119.64	18.12	7.38	-	-	0.51	4.17	26.69	-	-
8	Hausa Quarters, Abakaliki	6^0 17^{l} 47^{ll} 8^0 05^{l} 41^{ll}	382.31	18.79	25.82	1227.5	-	-	1.66	2.64	36.56	-	-
9	Obama Village, Abakaliki	6^0 18^{l} 36.3^{ll} 8^0 08^{l} 15.5^{ll}	147.62	31.05	34.35	251.32	-	-	2.15	10.54	73.61	-	-
10	Near Ejeke PS, Amasiri	5^0 55^{l} 29.8^{ll} 7^0 52^{l} 59.2^{ll}	73.28	40.69	0.35	50.15	11.86	-	0.85	7,27	0.92	57.35	-
11	Comm. Sec. Sch. Abomege	6^0 01^{l} 10.7^{ll} 8^0 00 ^{l} 21.1^{ll}	81.46	24.63	327.9	-	-	-	0.79	30.75	-	-	-
12	Fishermen PS Akpoha	5^0 58^{l} 17.3^{ll} 7^0 57^{l} 10^{ll}	228.15	95.53	32.73	2245.80	-	-	2.22	23.75	34.74	-	-
13	Amauda Ohofia Agba	6^0 18^{l} 26.4^{ll} 7^0 51^{l} 25.4^{ll}	328.15	32.12	20.67	44.29	11.72	-	0.77	0.24	8.21	24.82	-
14	Akpoha Central School	5^0 57^{l} 52.9^{ll} 7^0 58^{l} 0.3^{ll}	396.39	10.44	570.47	179.37	14.46	1142	1.6	0.43	3.36	20.68	2.94
15	St. Benedict Primary School, Imina	5^0 59^{l} 12.4^{ll} 8^0 01^{l} 0.15^{ll}	29.156	594.17	917.73	4.38	549.69	-	0.32	5.59	12.27	1.21	-
16	Near Ukawu water scheme	6^0 00^{l} 52.2^{ll} 7^0 57^{l} 52.3^{ll}	343.66	372.09	97.48	1.76	-	-	1.69	7.77	127.28	-	-
17	Amike Aba	6^0 20^{l} 40^{ll} 8^0 05^{l} 55^{ll}	1440.2	17.11	66.51	-	-	-	1.31	29.92	-	-	-
18	Odunukwe, St. Abakaliki	6^0 18^{l} 45^{ll} 8^0 05^{l} 14^{ll}	204.55	812.08	228.81	4107	-	-	0.14	4.93	93.81	-	-
19	Amasiri road, Ibii	5^0 55^{l} 22.5^{ll} 7^0 54^{l} 13.3^{ll}	192.65	2.22	258.55	-	-	-	1.95	0.28	-	-	-
20	Ozaraukwu, Amasiri	5^0 55^{l} 11.19^{ll} 7^0 54^{l} 36^{ll}	182.6	6.79	15,743	4.27	-	-	2.12	3.28	136.05	-	-
21	Central School, Amasiri	5^0 54^{l} 37.5^{ll} 7^0 53^{l} 22.9^{ll}	44.59	27.06	-	-	-	-	-	-	-	-	-

VES points		Latitude Longitude	ρ_1	ρ_2	ρ_3	ρ_4	ρ_5	ρ_6	h_1	h_2	h_3	h_4	h_5
22	Amike Aba, Abakaliki	6^0 21^{I} 12^{II} 8^0 06^{I} 37^{II}	78.14	8.31	20.73	12.98	-	-	1.01	1.59	2.44	51.24	-
23	Mgbabor, Abakaliki	6^0 20^{I} 25.1^{II} 8^0 04^{I} 59^{II}	419.22	1005.1	21.90	-	-	-	0.29	1.70	-	-	-
24	Presco Campus, EBSU (2)	6^0 19^{I} 27.7^{II} 8^0 04^{I} 53.5^{II}	242.1	67.47	0.66	93.55	9.27	-	1.46	1.25	0.24	14.12	-
25	Umuogudu Amankalu Oshiri	6^0 07^{I} 36^{II} 7^0 54^{I} 29^{II}	139.31	598.64	193.43	125.18	-	-	0.43	49.64	89.43	125.18	-
26	Azugwu, Abakaliki	6^0 19^{I} 42^{II} 8^0 07^{I} 41^{II}	1053.8	212.07	139.72	7926.30	-	-	2.69	10.50	44.37	-	-
27	Enuagu CPS, Onicha	6^0 05^{I} 05^{II} 7^0 48^{I} 42^{II}	151.28	4.98	-	-	-	-	-	-	-	-	-
28	Ahia Nkwo market, Okposi	6^0 03^{I} 26^{II} 7^0 47^{I} 50^{II}	177.91	51.03	-	-	-	-	-	-	-	-	-
29	Isiama Health Centre, Onicha	6^0 03^{I} 53^{II} 7^0 49^{I} 00^{II}	201.29	1630.70	75.37	-	-	-	0.41	1.42	-	-	-
30	Aja Nwachukwu PS, Okposi	6^0 03^{I} 45^{II} 7^0 48^{I} 29^{II}	304.19	18.84	80.99	-	-	-	3.57	8.25	-	-	-
31	FGC, Okposi	6^0 02^{I} 12^{II} 7^0 48^{I} 23^{II}	191.08	4.63	39.41	-	-	-	2.10	3.17	-	-	-
32	Holy Rosary PS, Okposi	6^0 02^{I} 16^{II} 7^0 48^{I} 23^{II}	491.56	184.56	2.15	112.11	1.11	-	1.12	5.22	0.51	22.25	-
33	Community High School Uburu	6^0 02^{I} 21^{II} 7^0 45^{I} 21^{II}	303.19	75.30	85.61	146.71	16.95	-	1.38	0.67	2.92	13.33	-
34	Inyimagu Azuiyiokwu, Abakaliki	6^0 18^{I} 12^{II} 8^0 07^{I} 48^{II}	125.59	161.89	11.77	-	-	-	2.31	6.37	-	-	-
35	Oferekpe Agbaja, Izzi	6^0 34^{I} 13^{II} 8^0 12^{I} 40^{II}	535.53	608.83	107.33	-	-	-	1.20	0.62	-	-	-
36	Perm. Site, EBSU	6^0 23^{I} 46^{II} 8^0 01^{I} 05^{II}	193.77	20.00	34.45	1480.60	-	-	1.67	4.21	38.14	-	-
37	Nwanu CPS, Izzi	6^0 28^{I} 33.2^{II} 8^0 14^{I} 11^{II}	3949.3	83.48	3.55	36.82	-	-	0.88	3.55	1.86	-	-
38	Boys Secondary school, Iboko	6^0 24^{I} 59.6^{II} 8^0 14^{I} 23.7^{II}	445.32	360.70	48.18	6039.60	-	-	0.32	4.99	36.66	-	-
39	Nwanphogu village, Abakaliki	6^0 12^{I} 38^{II} 8^0 10^{I} 33^{II}	1431.8	106.61	44.12	28.33	3060.20	-	1.93	1.75	7.61	86.97	-
40	Umuoghara, Ezza North	6^0 17^{I} 26^{II} 8^0 01^{I} 24^{II}	1333.3	27.21	2515.20	-	-	-	0.47	24.55	_-	_-	-

Table 3
Aquifer Vulnerability Index (AVI), general vulnerability and protective capacity classes (After Stempvoort et al. 1993; Foster et al. 2002; Akpan et al. 2015)

IEC ()	Protective Capacity	GOD	Vulnerability Rating	Hydraulic Resistance (*HR*)	Vulnerability (AVI)
> 2.0	Strong	< 0.3	Low	0–10	Extremely vulnerable
1.1–2.0	Moderate	0.3–0.5	Moderate	10–100	High
0.1–1.0	Fair	0.5–0.7	High	100–1000	Moderate
< 0.1	Weak	> 0.7	Extreme	1000–10,000	Low
				> 10,000	Extremely low

$IEC = \sum_{i=1}^{n} \frac{h_i}{\rho_i}$ -------- Eq. 1

Hydraulic conductivity, $k = 386.40 R_{VD}^{-0.93283}$ ---- Eq. 2

$HR = \sum_{k=1}^{n} \frac{h_i}{k_i}$ ------ Eq. 3

4.0 Results And Discussion

The geoelectric sections in the area comprise mainly 4 layers. A few points have 1, 2, 3, and 5 layers respectively, while one location only has 6 geoelectric layers (Table 1). The resistivities and thicknesses of the first to fifth layers are 29.16–3,949.30 Ωm; 0.14–3.57 m, 4.98–1,630.70 Ωm; 0.21–49.64 m, 0.35–3,767.20 Ωm; 0.24–89.43 m, 1.76–7926.30 Ωm; 1.21–125.18 m, and 1.11–3,060.20 Ωm respectively. The single sixth layer has a resistivity value of 1142 Ωm and an undefined thickness. Integration of the geoelectric sections with their borehole lithologs enabled the classification of the subsurface layers into topsoil, baked shale, fractured shale/sandstone (the aquiferous unit), and the consolidated sandstone units. The aquifer zone exists mostly between layers 3 and 4. Within the aquiferous zones, a resistivity range of ≤ 52 Ωm implies fractured shale aquifer while those > 52 ≤ 200 Ωm is fractured sandstone (Obasi et al. 2021). The topsoil is predominantly laterite, silt, and silty-clay soils. Few clay zones exist below 10 m from the surface in a few locations. Where they exist, they have a very thin thickness. Mineralogy has a significant influence on the resistivity of rocks. Hence, an increase in the clay minerals in a rock brings about low resistivity (Christiansen et al. 2014); Uhlemann et al. 2017). The rocks understudy are predominantly shales which are primarily made of clay minerals. They ought to have low resistivity values but they are not. They have lost their popular resistivity characteristics due to the effect of a series of tectonic episodes that they have experienced (Benkhelil 1989). The high resistivity observed in the shale units is attributable to high induration of the rocks as a result of compaction and baking arising from burial history and low-grade metamorphism (Obiora and Umeji 2004) that the rocks encountered in the Santonian period, which altered their mineralogical composition (Obiora and Charan 2011) and increased their density (Obasi and Selemo 2018). The degree of water saturation is another factor that alters the bulk subsurface resistivities of rocks (Telford et al., 1990; Uhlemann et al. 2017), whereby decreasing saturation causes an increase in their resistivity. These rocks lost their fissility and laminations in most places, thereby losing their primary porosity (Obasi and Selemo 2018), occurring massively, and behaving more like an aquiclude than an aquitard. Hence, the resistivity values of ≤ 50 Ωm that implies clay lithology (Lowrie 2007) only represent it at shallow depths of < 10 m below the surface. At depths ≥ 10 m, the same resistivity range represents the fractured/weathered baked shale/mudstone aquiferous zone (Obasi et al. 2021). The fresh, unfractured baked shale units have relatively high resistivities (Table 1) that are unfamiliar with normal shale as a rock. In such conditions, the baked shale units are expected to provide reasonable protection to the underlying aquifer system if they have some reasonable thickness. The resistivity of the vadose zone (R_{VD}) ranges from 31.97–3,381.68 Ωm with a mean value of ± 346.96 Ωm (Table 2; Fig. 3). The highest R_{VD} occurred in the northwestern portion of the study area, within the younger sediments of the Eze-Aku Group and Awgu Formation, and around Iboko. The values did not follow any defined trend southwards to distinguish it between the sediments of the Asu River and Eze-Aku Groups. The occurrence of the least resistivity range (31.97–701.91 Ωm) across about 75% of the map area is an indication that the majority of the vadose zone is made up of argillaceous materials that have been deformed and are highly indurated. Around Iboko, Ntezi – Okpoto – Ezillo axes, the consolidated sandstones outcropped at the surface, giving rise to the higher resistivity ranges encountered.

The thickness of the vadose zone (h_{VD}) ranges from 5.07–37.69 m, with a mean thickness of about 17.85 m (Fig. 4a). Obasi et al. (2021) have earlier stated that the depth of groundwater in the study area is ≥ 18 m. The highest h_{VD} occurred within the sediments of the Eze-Aku Group in Ohofia Agba, Onicha Igboeze, and Amasiri areas. The Abakaliki urban has a h_{VD} of 18–25 m. The least h_{VD} occurs in the central portion of the study area, trending virtually northwest–southeast. The thickness of the vadose zone tends to increase in the southwest and northeast directions. A correlation of the lithologs from some drilled boreholes in the study area (Fig. 4b) indicates that the thickness of the vadose zone at VES 2, 7, 22, 24, 34, and 35 are 28.53, 21.82, 21.00, 18.60, 6.00, and 12.00 m respectively.

The integrated electrical conductivity (IEC) values in the area are very low, ranging from 0.003–0.850 *S* and having a mean value of 0.134 *S* (Fig. 5). The low value of IEC is a further indication that there is the absence of a thick pile of clay to protect the aquifer (Casa et al. 2008; Oseji et al. 2018). Hence, the rate of infiltration and pollution is enhanced by the absence of the thick clay layer. The values of the IEC indicate that the protective capacity of the vadose zone in the entire study area is weak to fair (see Table 3).

The hydraulic conductivity of the vadose zone (k_{VD}) ranges from 0.20–16.11 m/day, with a mean value of 3.78 m/day (Fig. 6). The values are relatively high compared with normal argillaceous materials (Gens 2013). They are closer to sandy materials than argillaceous materials. This could be attributed to the fact that the topsoil is predominantly laterite, silt, and silty-clay soils, and some shale layers in the vadose zone are weathered/fractured (see Fig. 4b). In the absence of primary porosity in the shale layers, the effect of weathering and micro-fracturing enhanced high permeability in the vadose zone. The Least values of the k_{VD} occurred mostly in the northern portion of the map area with few occurring in the central and southern portion of the study area. The least k_{VD} occurred around Agbaja community with high h_{VD} but did not also occur in the southwestern portion of the map that has a similar range of h_{VD}. Again, the Abakaliki area that has a higher h_{VD} has a higher k_{VD} compared with the southeastern portion of the map. This is an indication that it is the soil type and presence of fracturing in the vadose zone and not its thickness that controls the protective capacity in the study area. The entire study area has high K_{VD} values, suggesting a high rate of infiltration into the aquifer zone.

The result of the hydraulic resistance (*HR*) in the study area (Fig. 7a) shows that its values range from 1.01–55.49 with a mean value of 9.96. *HR* depends on the thickness of the vadose zone and the nature of the geological material (Gemail et al. 2011). The majority of the study area has very low resistance to fluid flow. This is so because the thickness of the vadose zone is relatively thin, there is a near absence of a clay zone, and the k_{VD} is high. Hence, the effective porosity of the vadose zone is high (Kirsch 2006). An extensive impervious layer of a vadose zone that has a thin thickness and is fractured has been

previously associated with low aquifer protective capacity (Akpan et al. 2015). These are indications that the aquifer systems in the study area are highly at risk of pollution from the surface pollutants. Based on the vulnerability classes (Table 3), the central to the southern portion of the map area is extremely vulnerable, while the northern portion is highly vulnerable. The vulnerability agrees with even the degree of fracturing in the area. The southern portion tends to be more fractured than the north.

All the GOD values are greater than 0.7 which indicates that the study area is highly vulnerable to contamination (Fig. 7b). The Vulnerability rating based on the GOD is extreme.

The result of heavy metal analyses of some groundwater samples in the study area (Table 4) indicates that such heavy metals as As, Zn, Ni, total Fe, Cd, and Mn are above the maximum permissible limits for potable drinking water. Part of the pollutants is of anthropogenic origin (Omaka et al. 2017), arising from infiltrations of effluents from mining and agricultural practices. The water samples are predominantly hosted in the Asu River Group shales in the Abakaliki area. The result of the geochemistry of the Asu River Group shales (Table 5) indicates that there is a low concentration of Ni, Fe, and Mn in the host rocks, while As and Cd are absent. The high rate of the aforementioned heavy metals in the groundwater system is in no doubt of anthropogenic source. This is a further indication that the aquifer system is poorly protected and highly vulnerable to pollution.

Table 4
Heavy metal analyses data of some groundwater samples in the study area (After Omaka et al. 2017)

S/No	Location	Northing	Easting	As (Mg/l)	Cu (Mg/l)	Pb (Mg/l)	Zn (Mg/l)	Ni (Mg/l)	Fe^{+} (Mg/l)	Cd (Mg/l)	Mn (Mg/l)
1	Kpirikpiri Abakaliki	6.378	7.725	1.069	0.004	0.001	0.008	0.003	0.102	0.004	0.190
2	Odunukwe, Abakaliki	6.286	7.732	0.842	0.004	0.001	0.006	0.004	0.334	0.063	0.004
3	Former timber Shed, Abakaliki	6.251	7.718	0.815	0.004	0.001	4.156	0.003	0.352	0.005	0.004
4	Amike-Aba, Abakaliki	6.345	7.843	0.896	0.005	0.001	0.004	0.003	0.293	0.174	0.924
5	Abakaliki LG. Hqrs, Nkaliki	6.213	7.601	0.529	0.005	0.001	6.297	0.005	0.037	0.005	8.195
6	Mile 50, Abakaliki	6.308	7.588	0.913	0.004	0.001	0.010	0.004	0.360	0.065	2.061
7	Olisaemeka Street, Abakaliki	6.284	7.857	2.000	0.004	0.002	2.180	0.004	0.147	0.005	3.498
8	Hausa quarters, Abakaliki	6.250	7.511	0.966	0.003	0.002	0.007	0.003	0.007	0.079	0.005
9	Liberation Estate, Abakaliki	6.292	7.513	0.697	0.006	0.010	0.004	0.003	0.322	0.013	3.161
10	St. Michael Agbaja	6.281	7.735	1.771	0.004	0.010	0.560	0.004	0.211	0.161	0.252
11	St. Joseph's Lodge, Mgbabor	7.275	7.662	1.420	0.003	0.001	0.009	0.003	0.272	0.007	0.006
12	Ochudo City, Abakaliki	6.244	7.842	0.875	0.005	0.002	4.110	0.004	0.319	0.568	4.648
13	Alozie Street, Abakaliki 1	6.221	7.681	3.947	0.006	0.002	0.006	0.004	0.310	0.081	2.785
14	Ogbaga road, Abakaliki	6.502	7.754	0.707	0.012	0.002	10.088	0.012	0.203	0.487	1.671
15	Onunwafor, Abakaliki	6.188	7.778	1.096	0.017	0.002	0.010	0.011	0.697	0.176	0.004
16	Ogueru, Abakaliki 1	6.247	7.719	1.993	0.006	0.002	1.735	0.017	0.197	0.112	0.310
17	Onueke 1	6.202	7.661	3.694	0.002	0.005	0.204	0.005	0.173	0.007	3.694
18	Onueke 2	6.088	7.748	2.052	0.003	0.002	0.006	0.005	0.275	0.218	0.004
19	Onueke 3	6.062	7.706	1.298	0.004	0.002	3.928	0.006	0.360	0.243	0.082
20	Onueke 4	6.060	7.718	2.052	0.004	0.002	0.005	0.005	1.005	0.135	0.086
21	Onueke 5	5.995	7.602	2.083	0.004	0.002	0.004	0.004	0.090	0.356	0.086
22	Onueke 6	6.002	7.683	2.000	0.006	0.002	0.006	0.016	0.310	0.008	2.035
23	Ogueru Abakaliki 2	6.204	7.752	1.334	0.003	0.002	0.009	0.016	0.116	0.280	0.003
24	Alozie Abakaliki 2	6.201	7.747	2.122	0.007	0.005	0.006	0.003	0.433	0.306	3.406
25	Afia ochie Uburu	5.817	7.684	2.500	0.004	0.002	0.009	0.005	0.064	0.637	1.855
26	Onu Ogudu Uburu	5.825	7.722	2.710	0.010	0.001	0.006	0.003	0.008	0.466	5.180
27	Ogudu primary school Uburu	5.783	7.604	2.410	0.006	0.001	0.005	0.003	0.167	0.295	6.443
28	Obodoma Village square Okposi	5.824	7.708	1.930	0.010	0.001	2.673	0.007	0.178	0.006	0.4533
29	Ivi ezuzor, Okposi Okwu	5.722	7.524	1.610	0.009	0.002	0.010	0.003	0.144	0.218	4.674
30	Court area Okposi	5.718	7.681	1.420	0.005	0.002	0.009	0.005	0.007	0.271	4.558

Table 5
Major-element oxides (in weight percentage) and trace-element concentrations (in ppm) of the rocks from the Asu River group in Abakaliki area

(Adapted from Obiora and Charan, 2011)

	8S	9S	10S	15S	24S	28S	30S	31S	32S	36S	UCC
SiO_2	57.03	57.64	54.02	39.63	57.98	48.55	44.62	54.54	54.04	40.25	65.9
TiO_2	1.24	1.01	1.17	0.53	1.14	1.57	0.67	1.24	1.14	0.62	0.7
Al_2O_3	18.03	19.21	18.05	12.74	19.01	20.37	14.78	21.31	20.53	13.3	15.2
Fe_2O_3	6.82	8.26	10.62	4.48	10.25	7.55	5.81	10.07	10.58	5.33	4.0
MnO	0.02	0.04	0.14	0.06	0.12	0.05	0.12	0.04	0.17	0.07	-
MgO	1.04	2.35	1.88	1.42	1.58	1.18	1.80	1.97	2.51	1.80	2.2
CaO	0.52	0.59	0.48	18.87	0.16	0.49	12.24	0.17	0.68	19.07	4.2
Na_2O	0.82	0.67	0.76	0.49	0.81	0.13	0.54	0.73	0.93	0.81	3.9
K_2O	4.06	2.42	2.93	2.33	2.92	1.24	2.92	3.43	3.81	2.26	3.40
P_2O_5	0.15	0.12	0.08	0.12	0.10	0.11	0.14	0.13	0.10	0.18	-
LOI	9.84	7.54	9.23	18.4	6.10	18.09	16.59	6.5	5.29	16.71	-
Total	**99.57**	**98.85**	**99.36**	**99.07**	**100.17**	**99.33**	**100.23**	**100.13**	**99.78**	**100.4**	**100**
CIA	72.94	80.03	77.32	25.29	79.89	89.28	35.98	80.32	74.87	25.70	-
Sc	24.935	19.925	18.642	14.905	21.58	17.709	15.842	23.545	21.715	15.811	13.6
Ni	43.31	34.632	38.402	33.817	89.216	45.747	31.863	55.649	38.523	35.047	44
Cu	34.092	23.367	22.400	25.853	27.764	23.931	27.698	29.255	32.963	29.501	25
Zn	187.281	134.035	1123.491	85.372	117.342	99.665	147.316	115.84	178.381	99.547	71
Pb	4.673	4.272	6.176	4.51	7.439	6.596	7.894	10.448	8.421	7.191	17

Conclusion

The appraisal of the protective capacity of the vadose zone in the study area indicates that the underlying aquifer system is highly vulnerable to contaminants from anthropogenic sources. Since the grounder is the primary source of potable water in the area, there is a need for government to establish a standard water treatment plant to reduce the chances of water-borne disease in the environment. Individuals who drill some private boreholes should be encouraged to treat them before drinking.

Declarations

Compliance with Ethical standards

Authors contribution statement: Ikenna A. Obasi, Jamilu B. Ahmed II, Godwin O. Aigbadon, Emmanuel K. Anakwuba, Ernest O. Akudo, and Nneka M. Onwa contributed in writing the manuscript. Jamilu B. Ahmed II drew the maps. Ikenna A. Obasi, Jamilu B. Ahmed II, Godwin O. Aigbadon, Emmanuel K. Anakwuba, Ernest O. Akudo, and Nneka M. Onwa participated in proofreading the manuscript.

Disclosure of potential conflict of Interest: The authors declare that there is no competing interest while carrying out this research.

Informed Consent: The article was written with the consent of all the authors.

Funding: The authors did not receive support from any organization for the submitted work.

Financial Interests: The authors declare they have no financial interests.

Data Availability: The data for this research is available but was not uploaded as part of this submission.

References

1. Akpan AE, Ebong DE, Emeka CN, (2015) Exploratory assessment of groundwater vulnerability to pollution in Abi, southeastern Nigeria, using geophysical and geological techniques. Environ Monit Assess. 187: 156 DOI 10.1007/s10661-015-4380-2

2. Aller L, Bennet T, Lehr JH, Petty RJ, Hackett G, (1987) DRASTIC: a standardized system for evaluating ground water pollution potential using hydrogeologic settings. US EPA, 600/2-87-035.
3. Benkhelil J (1989) The origin and evolution of the Cretaceous Benue Trough, Nigeria. J Afr Earth Sci 8:251–282. https://doi.org/10.1016/S0899-5362(89)80028-4.
4. Casas A, Himi M, Diaz Y, Pinto V, Font X, Tapias JC, (2008) Assessing aquifer vulnerability to pollutants by electrical resistivity tomography (ERT) at a nitrate vulnerable zone in NE Spain. Environmental Geology, 54, 515–520.
5. Civita M, De Maio M, (1997) SINTACS Un Sistema parametricoper la valutazione e la cartografia per la valutazione della vulnerabilit'a degli acquiferi all'inquinamento, Metodologia e automazione. Bologna: Pitagora Ed. 191.
6. Conrad J, Hughes S, Weaver J, (2002) Map production. In Zaporozec A. (Ed), groundwater contamination inventory: a methodological guide (pp. 75–98). International Hydrogeological Programme-VI, No 2, UNESCO.
7. Christiansen AV, Foged N, Auken E, (2014) A concept for calculating accumulated clay thickness from borehole lithological logs and resistivity models for nitrate vulnerability assessment. Jour. Appli. Geophy. 108, 69–77.
8. Chukwu A, Obiora SC (2014) Whole-rock geochemistry of basic and intermediate intrusive rocks in the Ishiagu area: further evidence of an orogenic setting of the Lower Benue rift, southeastern Nigeria. Turkish J Earth Sci 23:427–443
9. Chukwu A, Obiora SC (2018) Geochemical constraints on the petrogenesis of the pyroclastic rocks in Abakaliki basin (Lower Benue Rift), Southeastern Nigeria. J Afr Earth Sci 141:207–220. DOI:10.1016/j.jafrearsci.2018.02.017
10. Draoui M, Vias J, Andreo B, Targuist K, and Stitou el Messarl J, (2007) A comparative study of four vulnerability mapping methods in a detritic aquifer under the medriterranean climatic conditions. Environmental geology, 54, 455–463.
11. Ducci D, Sellerino M, (2012) Vulnerability mapping of groundwater contamination based on 3D lithostratigraphical models of porous aquifers. Journal of Science of the Total Environment, 447, 315–322.
12. Ebokaiwe AP, Omaka ON, Okorie U, Oje O, Egedeigwe C, Ekwe A, Nnaji NJ, (2018) Assessment of heavy metals around Abakaliki metropolis and potential bioaccumulation and biochemical effects on the liver, kidney, and erythrocyte of rats, Human and Ecological Risk Assessment: An International Journal, DOI: 10.1080/10807039.2017.1410695
13. Ebong DE, Akpan AE, Onwuegbuche AA (2014) Estimation of geohydraulic parameters from fractured shales and sandstone aquifers of Abi (Nigeria) using electrical resistivity and hydrogeologic measurements. J Afr Earth Sci 96:99–109. https://doi.org/10.1016/j.jafrearsci.2014.03.026
14. Edet, A. E. (2014). An aquifer vulnerability assessment of the Benin Formation aquifer, Calabar, southeastern Nigeria, using DRASTIC and GIS approach. Journal of Environmental Earth Sciences, 71(4), 1747–1765.
15. Ezzy, T. R., Cox, M., O'Rourke, A. J., & Huftile, G. (2006). Groundwater flow modeling within a coastal alluvial plain setting using a high-resolution hydrofacies approach: Bells Creek plain, Australia. Hydrogeology Journal, 14, 675 – 688.
16. Famiglietti JS (2014) The global groundwater crisis. Nat Clim Change 4(11):945–948.
17. Foster, S. (1987). Fundamental concepts in aquifer vulnerability, pollution risk and protection strategy. In W. Van Duijvenbooden & H. G. Van-Waegeningh (Eds.), Vulnerability of soil and groundwater to pollutants (pp. 69– 86). The Hague: Hydrological Research.
18. Foster, S. S. D., Hirata, R., Gomes, D., D'Elia, M., & Paris, M. (2002). Groundwater quality protection: a guide for water utilities, municipal authorities and environment agencies (second ed.). Washington, DC: World Bank.
19. Fraga, C. M., Fernandes, L. F. S., Pacheco, F. A. L., Reis, C., & Moura, J. P. (2013). Exploratory assessment of groundwater vulnerability to pollution in the Sordo River Basin, Northeast of Portugal. REM: R. Esc. Minas, Ouro Preto, 66(1), 49–58.
20. Gens A, (2013) On the hydromechanical behaviour of argillaceous hard soils-weak rocks. Proceedings of the 15th European Conference on Soil Mechanics and Geotechnical Engineering – Geotechnics of Hard Soils – Weak Rocks (Part 4) A. In: Anagnostopoulos et al. (Eds.). 71–118. doi:10.3233/978-1-61499-199-1-71
21. Javadi, S., Kavehkar, N., Mousavizadeh, M. H., & Mohammadi, K. (2011).ModificationofDRASTICmodel tomapgroundwatervulnerabilitytopollutionusingnitratemeasurementsin agricultural areas. Journal of Agricultural Science and Technology, 13(2), 239–249.
22. Kirsch, R., Sengpiel, K., & Voss, W. (2003). The use of electrical conductivity mapping in the definition of an aquifer vulnerability index. Near Surface Geophysics, 1,3 – 20.
23. Leone, A., Ripa, M.N., Uricchio,V., Dek,L.,&Vargay,Z.(2009). Vulnerability and risk evaluation of agricultural nitrogen pollution for Hungary's main aquifer using DRASTIC and GLEAMS models. Journal of Environmental Management, 90(10), 2969–2978.
24. Lowrie, W (2007) Fundamentals of geophysics. Cambridge University Press, USA.
25. Murat RC, 1970. Stratigraphy and Palaeogeography of Cretaceous and Lower Tertiary in Southern Nigeria. 1st Conference on African Geology, Ibadan Proceedings. Ibadan University Press.
26. Obasi AI, Selemo AOI (2018) Density and reservoir properties of Cretaceous rocks in southern Benue Trough, Nigeria: implications for hydrocarbon exploration. Arab J Geosci 11:307. https://doi. org/10.1007/s1251 7-018-3634-z
27. Obasi AI, Onwa NM, and Ezekiel OI (2021) Application of the resistivity method in characterizing fractured aquifer in sedimentary rocks in Abakaliki area, southern Benue Trough, Nigeria. Envi. Earth Sci. 80:24. https://doi.org/10.1007/s12665-020-09303-w
28. Obiora SC, Charan SN (2011) Geochemistry of regionally metamorphosed sedimentary rocks from the lower Benue Rift: implications for provenance and tectonic setting of the Benue Rift. S Afr J Geol 114(1):25–40. doi:10.2113/gssajg.114.41

29. Obiora SC, Umeji AC (2004) Petrographic evidence for regional burialmetamorphism of the sedimentary rocks in the lower Benue rift. J Afr Earth Sci 38:269–27. doi:10.1016/j.jafrearsci.2004.01.001
30. Obiora DN, Ibuoti JC, George NJ (2016) Evaluation of aquifer potential, geoelectric and hydraulic parameters in Ezza North, southeastern Nigeria, using geoelectric Sounding. Int J Environ Sci Technol 13:435–444. https://doi.org/10.1007/s1376 2-015-0886-y
31. Okeke PO, Sowa A, Selemo AO, Iheagwu MC (1987) The thickness of the Cretaceous sediments in the southern Benue Trough, Nigeria, its tectonic implications. In: Matheis Schandelmeier (ed) Current research in African earth sciences. Balkema, Rotterdam, pp 295–298
32. Okiongbo KS, Akpofure E, (2012) Determination of aquifer properties and groundwater vulnerability mapping using geoelectric method in Yenagoa City and its environs in Bayelsa State, South South Nigeria. Journal of Water Resource and Protection, 4, 354 – 362.
33. Omaka ON, Aghamelu OP, Ike-Amadi CA, Ofoezie RC, (2017) Assessment of the quality of groundwater from different parts of southeastern Nigeria for potable use. Environ Earth Sci. 76: 344. DOI 10.1007/s12665-017-6680-z.
34. Onwa NM, Obasi AI, (2022) Application of the 2D electromagnetic tomography in delineating groundwater zones in pre–Santonian fractured sedimentary rocks in Abakaliki area, southern Benue Trough, Nigeria. Arabian Journal of Geosciences. 15:261. https://doi.org/10.1007/s12517-022-09443-2.
35. Raji WO, Abdulkadir KA (2020) Evaluation of groundwater potential of bedrock aquifers in Geological Sheet 223 Ilorin, Nigeria, using geo–electric sounding. Appli. Water Sci. 10(220): 1–12. https://doi.org/10.1007/s13201-020-01303-2
36. Sinkevich MG, Walter MT, Lembo AJ. Jr, Richards BK, Peranginangin N, Aburime SA, Steenhuis TS, (2005). A GIS-based ground water contamination risk assessment tool for pesticides. Ground Water Monitoring & Remediation, 25(4), 82–91.
37. Telford WM, Geldart LP, Sheriff RE (1990) Applied geophysics. Cambridge Univ. Press, 860p
38. Uhlemann S, Kurasa O, Richards RA, Naden E, Polya DA, (2017) Electrical resistivity tomography determines the spatial distribution of clay layer thickness and aquifer vulnerability, Kandal Province, Cambodia. Journal of Asian Earth Sciences. 147, 402–414.
39. Yin L, Zhang E, Wang X, Wenninger J, Dong J, Guo L, Huang J, (2012) A GIS-based DRASTIC model for assessing groundwater vulnerability in the Ordos Plateau, China. Environmental Earth Sciences, 69(1), 171–185.

Figures

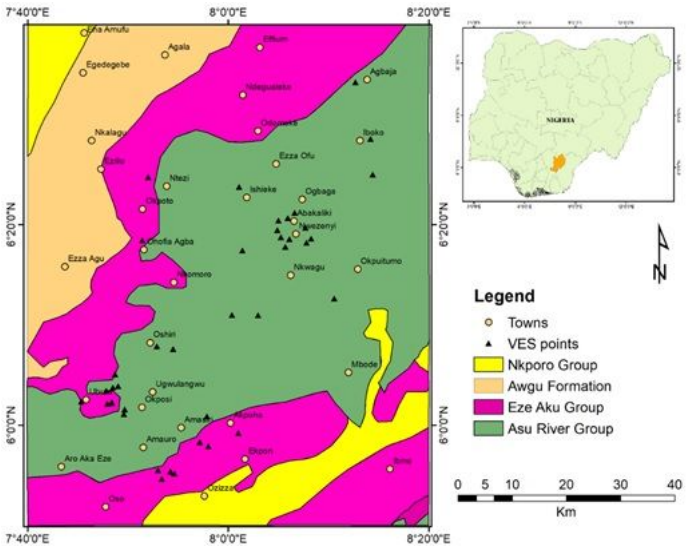

Figure 1

The Geological map of the study area.

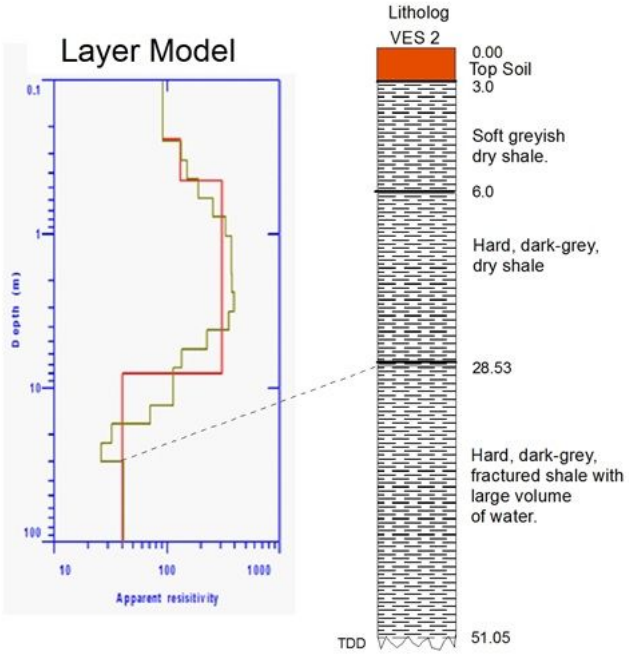

Figure 2

Determination of the thickness of the vadose zones from borehole logs and geoelectric sections (After Obasi et al. 2021)

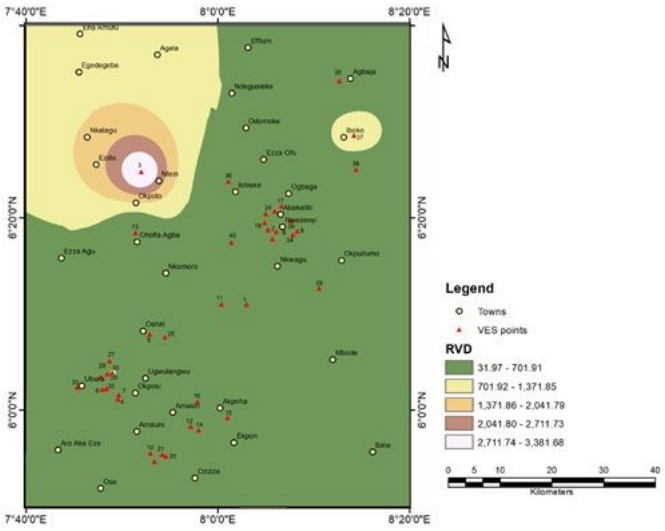

Figure 3

Map of the resistivity of the vadose zone across the study area.

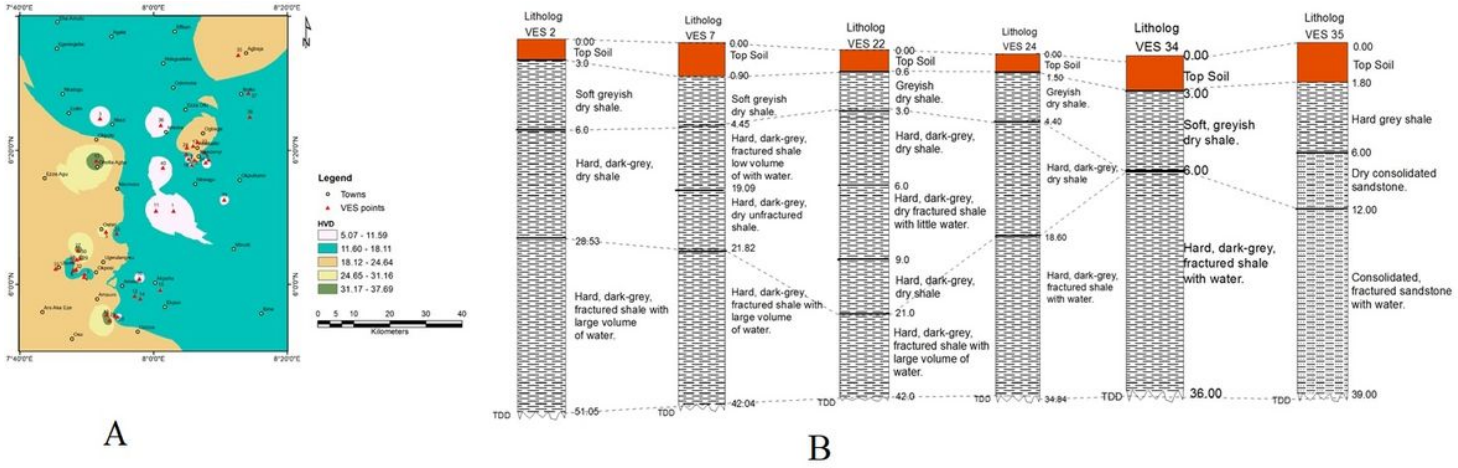

Figure 4

Thickness of the vadose zone in the strudy area. a: Map of the thickness of the Vadose zone in the study area. b: Correlation of thickness of the vadose zone across some drilled boreholes in the strudy area.

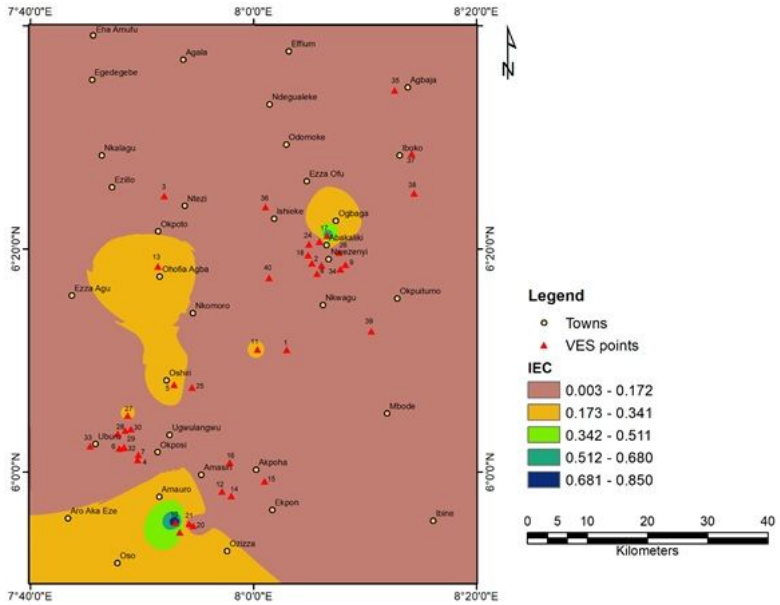

Figure 5

The IEC map of the study area

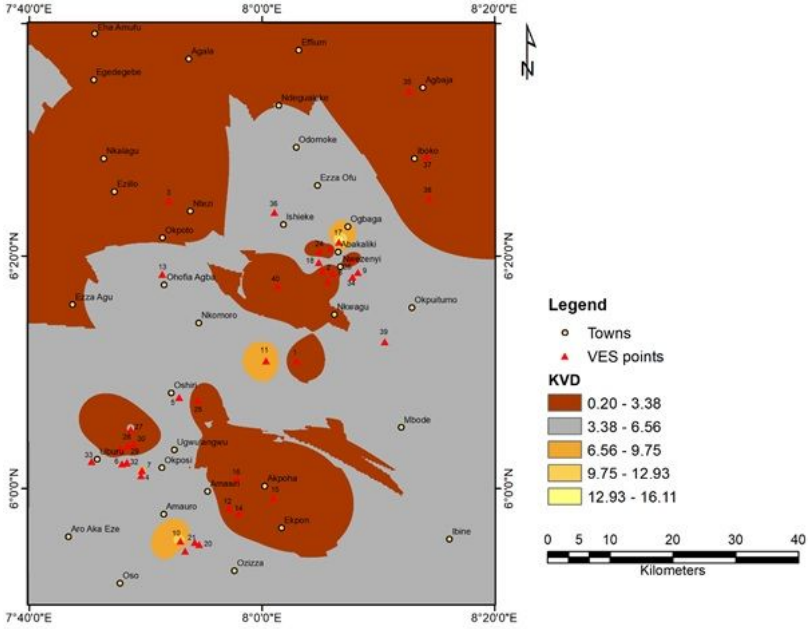

Figure 6

Map of the Hydraulic conductivity of the vadose zone in the study area.

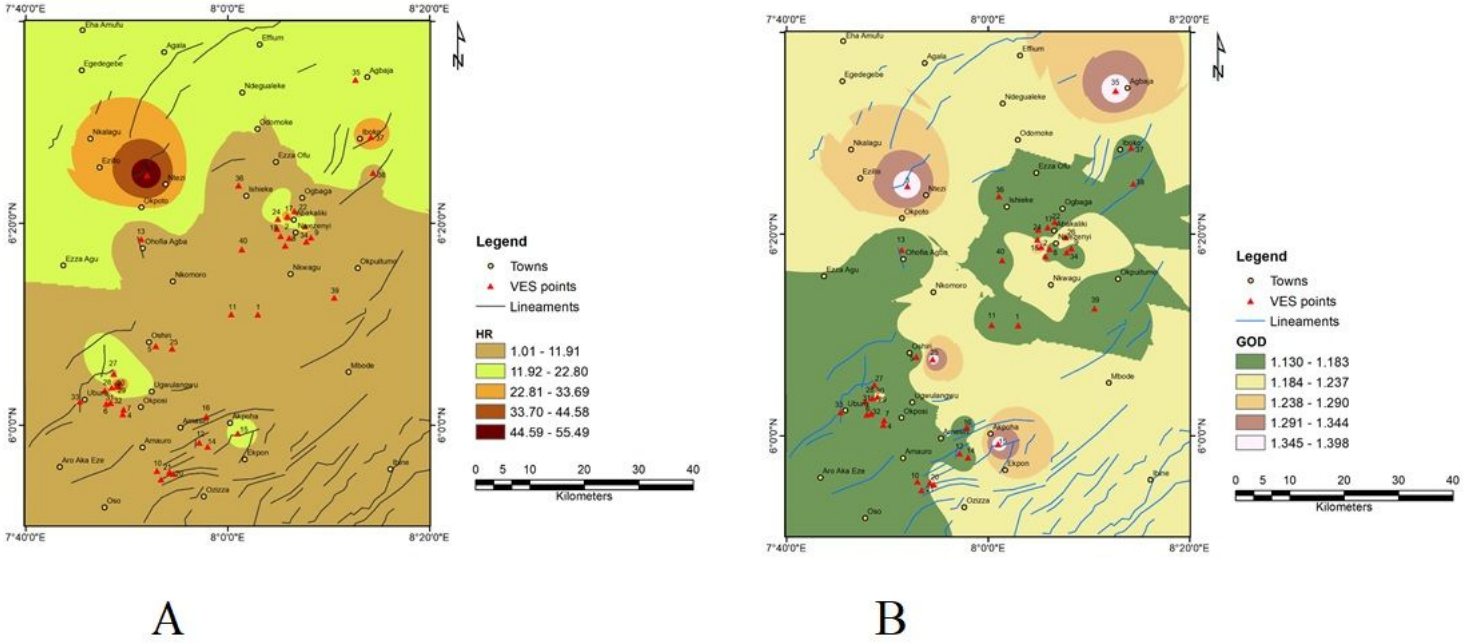

Figure 7

Vulnerability classification maps of the study area. a: Map of the hydraulic resistance of the vadose zone. 7b: GOD map of the study area.